AN ABSTRACT OF THE THESIS OF

Jeffrey Boyd for the degree of
Master of Science in Exercise and Sport Science
presented on April 6, 2006.
Title: Effect of the Calpain Inhibitor E-64-d on the Degradation of α-fodrin in Damaged Muscle

Abstract approved:

_____

Jeffrey J. Widrick

We hypothesized that calpain activity is elevated in response to muscle damage. To test this hypothesis, we examined the degradation of α-fodrin into its 150 and 145 kDa fragments following either 20 eccentric or isometric contractions. In addition, experiments were performed in the presence or absence of E-64-d, a calpain inhibitor. Both EDL and SOL muscles displayed significant differences ($p<0.003$ and $p<0.002$ respectively) between the raw and normalized 150 and 145 kDa α-fodrin fragments of the DMSO + E-64-d compared to the other bath treatments. Based on our model of exercise-induced muscle damage, we expected to see greater levels of 150 and 145 kDa α-fodrin fragments in those muscles that performed the eccentric protocol. However, there was no evidence that eccentric muscle damage increased the levels of 150 and 145 kDa α-fodrin fragments over the levels observed in the isometric trials. These findings suggest that the magnitude of damage was insufficient to activate calpains.

Effect of the Calpain Inhibitor E-64-d on the Degradation of α-fodrin in Damaged Muscle

by
Jeffrey Boyd

A THESIS

submitted to

Oregon State University

in partial fulfillment of
the requirements for the
degree of

Master of Science

Presented April 6, 2006
Commencement June 2006

Master of Science thesis of Jeffrey Boyd presented on April 6, 2006

APPROVED:

_____

Major Professor, representing Exercise and Sport Science

_____

Chair of the Department of Nutrition and Exercise Science

_____

Dean of the Graduate School

I understand that my thesis will become part of the permanent collection of Oregon State University libraries. My signature below authorizes release of my thesis to any reader upon request.

_____

Jeffrey Boyd, Author

ACKNOWLEDGEMENTS

The author expresses sincere appreciation to all those who contributed to this project. A special thanks to Dr. Ho who allowed the use lab equipment for Western blotting and to Dr. Bella who provided insight and protocol suggestions regarding the Western blotting process. Thanks to Tyler Barker for his assistance in data collection, and to the Department of Nutrition and Exercise Science for their funding to cover supplies.

TABLE OF CONTENTS

LIST OF FIGURES

LIST OF TABLES

LIST OF TABLES (Continued)

Effect of the Calpain Inhibitor E-64-d on the Degradation of α-fodrin in Damaged Muscle.

Introduction

Skeletal muscle is capable of three different types of contractions: isometric contractions, in which muscles produce force but do not change in length, concentric contractions, in which muscles produce force while shortening in length, and eccentric contractions, in which muscles produce force while lengthening. Combinations of these contractions are used during movement and other physical activities. While muscle fibers can be damaged by acute trauma, damage most frequently occurs during eccentric contractions. Eccentric contractions are quite common, as muscles dissipate energy, absorb shock, and slow limb movements. The resulting muscle damage is closely associated with swelling, inflammation, soreness, and prolonged weakness. These symptoms, of varying degrees of intensity, tend to subside after about seven days following the initial damaging event.

Histologically, damaged muscles show destruction and disarray of the cell ultrastructure, characterized by Z-band streaming, the loss of register between A-bands, and the shearing of t-tubules from the sarcolemma. These observations suggest damage or degradation to force-bearing proteins comprising the Z-bands, to intermediate filaments such as desmin that maintain alignment between myofibrils, to titin, a protein that serves to position the A-band in the center of the sarcomere, and to

the costameric structures involved in the transmission of force from the myofibrils across the sarcolemma.

Damage to the t-tubules and the sarcolemma allows normally impermanent ions entry into the cell. This is believed to be related to an increase in resting intracellular calcium levels within the damaged cell. The calcium-activated protease calpain is located in or around the Z-band regions. Once activated by calcium, calpains display limited but highly specific proteolytic activity. At least *in vitro,* calpains target many cytoskeletal proteins, including α-fodrin, desmin, dystrophin, and titin. These proteins are cleaved at a limited number of very specific sites. Thus, calpains are thought to initiate disassembly of the sarcomere in response to increased intracellular calcium.

Because eccentric contractions are known to increase permeability to calcium and to disrupt intracellular calcium homeostasis, we hypothesize that calpains are activated in damaged muscle cells. Thus, calpains may be directly involved in Z-band disruption and loss of myofibrillar alignment, several of the key early events in muscle damage. However, evidence in support of this hypothesis is lacking.

One particular target of the calpains is the Z-line and costameric protein α-fodrin. The degradation of α-fodrin by calpain produces two distinct peptide fragments. Because these fragments retain their immuno-reactivity to antibodies against intact α-fodrin, they have been used as an index of *in vivo* calpain-mediated proteolysis in cardiac muscle preparations and in cell culture systems.

In this study, we will test the hypothesis that calpains are activated under the *in vitro* conditions present following contraction-induced muscle damage. Our approach

will utilize isolated muscles, subjected to isometric or eccentric contractions, in the presence or absence of the calpain inhibitor E-64-d. The breakdown of α-fodrin will be used as an index of *in vitro* calpain-mediated proteolysis. We hypothesize that those muscles performing eccentric contractions will exhibit more breakdown of α-fodrin compared to those muscles performing isometric contractions, and that this breakdown after eccentric exercise will be reduced in the presence of E-64-d.

Literature Review

Exercise-Induced Muscle Damage

Skeletal muscles perform multiple modes of contraction that are characterized by changes in muscle length during the generation of force. An isometric contraction occurs when the muscle contracts to produce tension yet there is no change in the length of the muscle. An example of this type of contraction is when an individual tries to pick up an object beyond their capacity. Their muscles contract, producing force, but because the object does not move, the muscle does not shorten.

In a shortening, concentric, or miometric contraction, the muscle shortens to produce tension to overcome or move a resistance. An example of this type of contraction is when an individual picks up an object within their capacity. Their muscles are activated, producing force, and because the resistance is less then the muscle's maximum force, the muscles shorten and the individual is able to pick up the object.

The third and final type of contraction is a lengthening, eccentric, or plyometric contraction. With an eccentric contraction, the muscle contracts to produce force, yet the direction of limb movement opposes shortening. An example of this type of contraction is when an individual lowers a heavy object from overhead in a controlled manner. Their muscles are required to contract and generate force, yet as they lower the object from above their head, their contracted muscles are required to lengthen.

In summary, isometric contractions stabilize joints, concentric contractions produce the power necessary for limb rotation and movement, and eccentric contractions act to dissipate energy, absorb shock and slow limb movements. All physical activities are a combination of these three types of contractions.

It has been repeatedly shown that eccentric muscle activity is much more likely to induce injury and damage than either isometric or concentric contractions (3, 15, 21, 46, 47). A muscle fiber may undergo numerous isometric or concentric contractions with little to no effect on the fiber itself, yet damage occurs shortly after a muscle begins performing eccentric contractions. In both humans and animals, these injuries result in decreased force production, muscle swelling, inflammation, disrupted sarcomeres, prolonged muscle weakness, and catabolism of proteins, as well as the efflux of muscle proteins into the circulation and influx of molecules and ions into the damaged cell (13, 18, 37, 39, 45, 67-69, 74).

Muscle Structure

The structural hierarchy of skeletal muscle begins with each whole skeletal muscle composed of numerous fascicles, or bundles, of muscle fibers. Each individual muscle fiber is composed of numerous myofibrils arranged in parallel. These myofibrils are themselves composed of numerous sarcomeres arranged in series, separated by regions known as Z-bands (4, 31). Sarcomeres are composed of interdigitating thick and thin filaments. The sliding movement of the thick and thin filaments back and forth causes the shortening and lengthening of muscles (30-32). Six thin filaments surround one thick filament in a hexagonally arranged lattice and the globular heads of the thick filament extend to interact with the thin filaments, forming cross-bridges (4). The thick filaments slide past the thin filaments, causing the shortening or lengthening of the entire sarcomere without a change in length of either filament (30, 32).

The amount of force on each half of the thick filament is proportional to the number of cross-bridges formed between the overlapping thin filaments (25). With the thick filament located in the exact center of the sarcomere, each half sarcomere will be pulled equally in opposite directions. However, if the thick filament is not aligned in the center of the sarcomere, opposing half-sarcomeres will form unequal numbers of cross-bridges and the thick filament will be pulled towards the half-sarcomere with the greater number of cross-bridges. Thus, with thick filament misalignment, there is the possibility that sarcomere instability might occur upon muscle activation. Even a relatively small initial imbalance would be amplified as the thick filament is pulled further and further toward one end of the sarcomere (28).

Under normal conditions, the thick filament remains aligned within the sarcomere. If a solvent such as gelsolin is used to dissolve away the thin filaments in a muscle fiber revealing the underlying thick filament, it can be seen that these thick filaments are connected to the Z-bands by fine strands consisting of a large protein, titin (27, 28, 66). Titin spans half the sarcomere with one end of the strand firmly attached to the thick filament while the other end extends to the end of the sarcomere and the Z-band region (27). Because of their structure and position, each pair of titin strands function in opposition to act as longitudinal stabilizers for the thick filaments by keeping them in the center of the sarcomere during contraction and relaxation (4). The titin strands also act like springs and contribute much of the elasticity of the muscle fiber when it is stretched by external forces or by the shortening of unequal sarcomeres (4, 66).

The thin filaments receive positional support from their cross-bridges with thick filaments as well as their insertions into the Z-band (4). The Z-band contains numerous proteins, such as α-actinin, desmin, vimentin, synemin, titin, and α-fodrin. The protein makeup of the Z-band serves to anchor the thin filaments to the Z-band, link adjacent sarcomeres together in longitudinal or transverse axes, and transmit tension during muscle contraction (4).

Proposed Mechanisms of Contraction-Induced Muscle Damage

Exercise or contraction-induced muscle damage is associated with a decline in the force that a muscle is able to generate. This drop in force, cannot be attributed to fatigue, implicating some degree of damage to the muscle. Damage is thought to be

brought about by one of two mechanisms. The first mechanism deals with the overstretching of muscle sarcomeres, ultimately resulting in the presence of disrupted sarcomeres (45). The second mechanism deals with damage to the components of the excitation-contraction coupling (EC coupling) process (33).

The concept that the damage process begins with overstretched sarcomeres comes from Morgan's proposed injury sequence (45). Based on Gordon, Huxley, and Julian's model of the length-tension curve (24), as a sarcomere lengthens, it moves across the plateau phase and onto the descending limb of the length-tension curve where tension declines. It is proposed that during the active lengthening of a muscle, most of the length change will be taken up by the weakest sarcomere in the myofibril. The weakest sarcomere is stretched by the surrounding, stronger sarcomeres until the point where it moves beyond the plateau region onto the descending limb of its length-tension curve. Once on the descending limb, these sarcomeres will become increasingly weaker. Consequently, they will be stretched even more by the surrounding, stronger sarcomeres, causing a rapid lengthening of the weak sarcomere. At this stage, the sarcomere has been stretched to the point where the force production from any remaining cross-bridges is minimal, but tension rises because of the passive structures within the sarcomere. Once passive tension has equilibrated to that of the surrounding sarcomeres, the sarcomere is stable. However, the process is repeated with the next weakest sarcomere stretching, and so on.

At the end of the stretch, when the muscle relaxes, myofibrils in the majority of overstretched sarcomeres re-interdigitate so that they are able to resume their normal function. Those that do not re-interdigitate are termed disrupted sarcomeres.

During repeated eccentric contractions, the number of disrupted sarcomeres would continually grow. Morgan and his colleagues (45) contend that these non-interdigitating or "popped" sarcomeres initiate damage to the cell.

Data support the idea of nonuniform sarcomere length and sarcomere disruption during eccentric contractions. It has been shown that after a series of eccentric contractions, muscle sarcomeres become much more nonuniform in their length, causing a shift in the length-tension curve to the right, and a drop in tension development (13, 45, 74). These results support the idea that the initial event in an eccentric contraction, which may ultimately lead to fiber injury and degradation, is the overstretch of unstable sarcomeres.

An alternate view of the damage process entails impairment of EC coupling (6, 33, 71, 72). Excitation-contraction coupling is the series of events whereby neural input stimulates muscular contraction. The process begins with the release of acetylcholine by the α-motoneuron at the neuromuscular junction. The resulting action potential passes along the plasmalemma and down into the muscle fiber via the t-tubule. Depolarization of the t-tubule activates specialized voltage sensors, causing the release of calcium (Ca^{2+}) into the cytosol from the sarcoplamic reticulum (SR). In the cytoplasm, Ca^{2+} binds to troponin and the regulatory light chain to initiate cross-bridge cycling (71).

Three potential pathways have been implicated as sites of possible impairment of the EC coupling system: the plasmalemma, the t-tubules, and the SR. With damage to the plasmalemma, normal ion distribution would be altered causing adverse effects on action potential conduction (72). In order to investigate this possibility,

microelectrode measurements of resting membrane potential for muscles performing 20 eccentric contractions were compared to those of muscles performing 20 isometric contractions (72). The near identical results suggest that the membrane resting conductance was normal and the ability of injured fibers to conduct action potentials was not impaired.

In order to assess the potential impairment of the t-tubules, fibers can be exposed to solutions containing high concentrations of potassium (71). The high concentration of extracellular potassium acts to depolarize all membranes exposed to the extracellular space so that a site of action potential conduction blockage can be bypassed. If during the experiment, the drop in potassium-elicited force was less than the initial reduction in experimental force, the t-tubule membrane would be implicated as the failure site (71). Results show that injury reduced the high potassium-elicited force to the same extent as it did experimental force (71). Based upon these results, it appears that the failure site in the EC coupling pathway lies below the t-tubule membrane (71).

With both the plasmalemma and the t-tubule being ruled out as locations of impairment, the SR's ability to release and subsequently uptake Ca^{2+} comes into question. Caffeine and 4-chloro-*m*-cresol, act to increase the intracellular cytosolic Ca^{2+} concentration by promoting the release of Ca^{2+} from the SR. Because the force of eccentrically damaged muscles is restored by these substances, it has been concluded that the impairment must occur at or above the level of SR Ca^{2+} release (6, 33, 71, 72).

Based on these results, it appears that the failure site in the EC coupling pathway lies between the t-tubule voltage sensor and the SR Ca^{2+} release channel (71). Regardless of the exact mechanism, up to 75% of the displayed force deficit following injury can potentially be attributed to impairment of the EC coupling pathway (33, 71, 72).

Proteolysis as a Contributing Mechanism

Skeletal muscle is believed to contain multiple proteolytic pathways (60). It is a combination of several of these pathways which causes the breakdown of myofibrils once damaged.

Lysosomes are structures which contain a variety of hydrolytic enzymes capable of degrading cellular macromolecules (42). These enzymes, found to be expressed in a wide variety of cells, primarily degrade proteins non-selectively inside the lysosome (63). Therefore, in order for their degradative activity to occur, the cellular macromolecules must be transported into the lysosome. The routes for delivery of macromolucules to lysosomes are endocytosis, autophagy, the biosynthetic route, and the newly discovered "kiss and run" (42). However, lysosomal activity generally occurs too late to account for the loss of myofibrillar proteins immediately post-exercise (10), indicating the involvement of other pathways.

The ubiquitin (Ub)-proteasome pathway is the major non-lysosomal process responsible for housekeeping functions such as basal protein turnover and the elimination of abnormal proteins (60). This complex process involves two main steps. The first is the attachment of Ub to the desired protein. Only those proteins that are

tagged with a polyUb degradation signal consisting of at least four Ub moietics are recognized for the next step (60). The second step in the Ub-proteasome pathway is the degradation of the ployUb proteins by the 26S proteasome complex. These peptides are recognized by the 26S proteasome and degraded into peptides (60). The resulting peptides then undergo further hydrolysis into amino acids.

The rate limiting step in this process appears to be the disassociation of myofibrillar proteins from the myofibril (53). Purified myosin, actin, troponin, and tropomyosin are hydrolyzed rapidly by the Ub-proteasome pathway, however, these proteins are considerably more resistant to degradation by the proteasome when they are assembled into myofibrils or an actomyosin complex (53). Thus it would seem that the disassociation of myofibrilar proteins from the contractile filament is the rate-limiting step in this process (53). It appears that another mechanism, responsible for the disassembly of sarcomereic proteins and Z-band disintegration, may be acting upstream of the proteasome.

Ca^{2+}-Activated Proteolytic Enzymes

Calcium-activated neutral proteases consist of a family of proteolytic enzymes termed calpains, which are intracellular non-lysosomal cysteine proteases (10). Within the sarcomere, it has been shown that the various isoenzymes of calpains are mainly located on or next to the Z-band with smaller amounts in the I-band and very little in the A-band (10, 22, 51, 52, 54, 55). The precise mechanism by which calpains are activated is somewhat unclear. Calpain activity appears to be regulated by the binding of Ca^{2+} to specific sites on the calpain molecule which causes a response

specific for that site, such as proteolysis or the binding of calpastatin (23). However, in order for proteolytic activity to occur, the calpain molecule must first undergo autolysis. Calpain undergoes rapid autolysis in the presence of sufficient Ca^{2+}, and that autolysis lowers the intracellular Ca^{2+} required for proteolysis (52).

Once activated, calpain causes the selective proteolysis of various contractile, metabolic, and structural proteins (10, 39). It is important to note that the action of calpains is not to degrade proteins into small pepetides or amino acids. Rather, calpains cleave proteins at very specific sites resulting in the creation of large peptides (22, 52). These peptides must then undergo further hydrolysis into amino acids. It is plausible that calpains may be responsible for the initial disassembly of actin, myosin, and other proteins for more extensive degradation by other processes, such as the 26S proteasome.

Rise in Ca^{2+} After Exercise-Induced Muscle Damage

Alterations in resting free intracellular calcium ($[Ca^{2+}]_i$) homeostasis have been implicated in the process of skeletal muscle injury following damaging contractions (43). While transient changes in $[Ca^{2+}]_i$ are essential in the EC coupling process, sustained $[Ca^{2+}]_i$ increases may result in the activation of calpains (10). The increasing tension and subsequent damage to the sarcomere during eccentric contractions potentially allows extracellular Ca^{2+} ($[Ca^{2+}]_o$) to enter the cell through the Ca^{2+} channels in the sarcolemma, ruptures in the t-tubules, and/or ruptures in the cell membrane itself (3, 16, 74). Normally, organelles such as mitochondria, the SR,

and sarcolemma translocation mechanisms buffer against a rise in free cytostolic $[Ca^{2+}]_i$ (41). However, if the fiber's buffering capacity is exceeded, the $[Ca^{2+}]_i$ level should increase. The elevated $[Ca^{2+}]_i$ and activation of calpains would result in the degradation of contractile and non-contractile structures within the sarcomere, ultimately causing a progressive reduction in the sarcomere's physiological performance (22). These results would not just occur at the specific sites of damage, but would occur to the whole fiber as $[Ca^{2+}]_i$ levels are uniformly distributed along muscle fibers post-stretch (7).

Previous Work on Calpains and Striated Muscle Dysfunction

In heart models, ischemia and Ca^{2+}-overload have been associated with elevated Ca^{2+} levels and calpain activity (8, 34, 62, 75). In a study by Tsuji et al (62), hearts exposed to high levels of Ca^{2+} displayed increased proteolysis of the cytoskeletal protein α-fodrin, whereas other proteins were unaffected. Degradation of α-fodrin (240-kDa in heart tissue, 280-kDa in skeletal tissue) by calpain produces two distinct peptide fragments (150 and 145-kDa) (8, 61, 62, 75). These fragments retain their immuno-reactivity to an α-fodrin antibody and have been identified as the preferred method to indicate calpain-mediated proteolysis (22). Three times the amount of 150-kDa α-fodrin fragment was found in hearts reperfused with a solution containing a high concentration of Ca^{2+} (62). It was concluded that Ca^{2+} overloading during reperfusion caused calpain-mediated proteolysis of α-fodrin.

Yoshida et al (75) examined varying rates of ischemia followed by varying lengths of reperfusion with a Ca^{2+} containing solution. Results display an increase in

the 150-kDa α-fodrin fragment as the length of reperfusion increased up to thirty minutes, the experimental limit.

Protein Degradation After Exercise-Induced Muscle Damage

In contrast to cardiac muscle, very little is known about the role of calpains in skeletal muscle damage. Most evidence is circumstantial. Following exercise induced muscle damage, proteins such as α-actinin, plectin, α-fodrin, dystrophin, titin, and desmin (37, 39, 40, 64), all of which are calpain substrates (22), have been shown to be degraded. However, there is little evidence linking degradation of these proteins to calpain activity.

One of the few studies to examine the interactions of exercise and calpains was conducted by Belcastro (9). Belcastro examined calpain activity (both the low and high Ca^{2+} requiring isoenzymes, μ- and *m*-calpain respectively) in muscle homogenates prepared from rats run to exhaustion on a treadmill (9). Partially purified μ- and *m*-calpain containing fractions were combined with casein and Ca^{2+} to study proteolysis *in vitro*. Results indicated an increased activity of calpain taken from muscles of exercised animals versus control animals. The increased activity was also accompanied by a heightened Ca^{2+} sensitivity of the enzyme.

While this study shows that purified enzymes are more active when stimulated with supra-physiological levels of Ca^{2+}, it is difficult to extrapolate this finding to physiological conditions where Ca^{2+} levels are substantially less. Furthermore, the authors did not determine whether or not it was damaging exercise or simply exercise in general which caused the changes in calpain activity.

Calpain Inhibitors Reduce Muscle Degeneration

Mutations in the gene for dystrophin underlie the muscle degeneration that occurs in Duchenne muscular dystrophy (DMD) (14, 26). DMD pathologies are characterized by myofibrillar protein loss, Z-line disorganization, plasma membrane defects, and dilation of the SR (14). Abnormally high concentrations of $[Ca^{2+}]_i$ are found in DMD muscles, resulting from damage to the cell membranes (2, 11, 57). The relationship between the increased Ca^{2+} levels and the subsequent abnormalities suggest that calpains play a key role in degeneration and degradation in dystrophic muscle (56).

Several studies have examined the effect of calpain inhibitors in reducing muscle degeneration in muscular dystrophy, clearly implicating the involvement of the calpain system (59). This model, with leaky cell membranes and increased $[Ca^{2+}]_i$ is very similar to that seen in exercise-induced muscle damage. Thus, with very similar etiologies, calpain inhibitors should potentially reduce muscle degradation in exercise-induced muscle damage.

Calpain activity in dystrophic muscle decreased significantly and substantially in response to treatment with calpain inhibitors (5, 38, 59, 65). Untreated dystrophic myofibers in *mdx* mice were characterized by myofiber degeneration whereas increases in myofiber diameter were found in inhibitor-treated muscles (59).

Other studies have shown similar findings in regards to the use of calpain inhibitors (49, 50). Calpain inhibitors improved motorneuron survival and subsequent muscle function in rats following nerve injury (36). In the damaged heart muscle

studies previously discussed (62, 75), the use of a calpain inhibitors significantly suppressed the degradation of the Z-band protein α-fodrin.

Proposed research

We propose the following sequence of events in exercise-induced muscle damage. First, fiber strain produces sarcomere instability and/or EC coupling impairment. Secondly, these changes allow the influx of Ca^{2+} into the sarcomere. Third, the Ca^{2+} buffering capacity of the mitochondria and the SR is exceeded. Fourth, the $[Ca^{2+}]_i$ rises above physiologically normal levels. We hypothesize that increased $[Ca^{2+}]_i$ causes the activation of calpains, resulting in the selective hydrolysis or disruption of the intermediate filament network.

The purpose of this study is to test the hypothesis that calpain activity is elevated in response to muscle damage. We will test this hypothesis by examining the degradation of α-fodrin, a sensitive and specific calpain substrate, into its 150 and 145 k-Da fragments. In addition, experiments will be performed in the presence or absence of E-64-d, a calpain inhibitor. We predict that those muscles performing eccentric contractions will exhibit more breakdown of α-fodrin compared to those muscles performing isometric contractions, and that this breakdown after eccentric contractions will be reduced in the presence of E-64-d.

Methods

Animals

Male ICR mice, between 30 and 35 g body weight, were obtained from Harlan (Harlan Sprague Dawley, Indianapolis, IN). The mice had ad libitum access to both feed and water and were housed in a temperature controlled environment (22°C) with a 12 hour light/dark cycle. On the day of their study, the mice were transported to the experimental location. Mice were anesthetized with sodium pentabarbitol (40 mg/g body weight). Supplemental doses were administered as needed in order to inhibit a toe pinch response. All animal care and use procedures were approved by the OSU Institutional Animal Care and Use Committee.

In Vitro Muscle Preparation

An incision was made around the skin of the ankle, the skin retracted, and the extensor digitorum longus (EDL) and soleus (SOL) muscles exposed. EDL and SOL muscles were dissected and placed in a dish containing Krebs-Ringer perfused with 95% oxygen (O_2) and 5% carbon dioxide (CO_2). Silk suture was tied to the distal and proximal tendons of each muscle. One EDL or SOL muscle had its distal tendon attached to a fixed post and the proximal tendon securely attached to the lever arm of a dual mode muscle lever system (model 300B-LR, Aurora Scientific Inc., Aurora, Ontario Canada) with platinum stimulation electrodes running parallel to the muscle. The contrallateral EDL or SOL muscle had its distal tendon attached to a fixed post and the proximal tendon to an isometric force transducer (model AH60-2996, Harvard Apparatus, Holliston, MA) with platinum stimulation electrodes running parallel to the muscle. Once prepared, each muscle was carefully placed in a water-jacketed

chamber filled with approximately 3 ml of Krebs-Ringer bicarbonate buffer solution, continuously perfused with 95% O_2 and 5% CO_2. The outer water jacket of the chamber was connected to a circulating water bath in order to maintain the temperature of the Ringer at 35°C. This temperature was chosen because it is a physiological muscle temperature and Ca^{2+} accumulation in damage muscle is temperature dependent (70). The temperature of the Ringer was monitored continuously using a small thermocouple.

Krebs-*Ringer Solutions*

The modified Krebs-Ringer bicarbonate buffer solution that was used in this project contained 137 mM NaCl, 11 mM glucose, 5 mM KCl, 1.25 mM $CaCl_2$, 1 mM $MgSO_4$, 1 mM NaH_2PO_4, 24 mM $NaHCO_3$, and 0.025 mM tubocurarine chloride. A stock solution of E-64-d (Peptide Institute Inc., Osaka, Japan) was made by dissolving the inhibitor in DMSO (D2650, Sigma-Aldrich, St. Loius, MO). This stock solution was added to the standard Krebs-Ringer to give a second Krebs-Ringer solution with final E-64-d and DMSO concentrations of 120 μM and 0.6% respectively. A third Krebs-Ringer solution was made that contained 0.6% DMSO.

Measurement of Contractile Properties

Each muscle was allowed to equilibrate in the experimental solution for 20 minutes before establishing optimal length (L_o). In order to obtain L_o, each muscle was stimulated every 3 minutes with 200 μs square-wave pulses delivered at a frequency of 300-Hz for EDL muscles, and 200-Hz for SOL muscles. Train duration was 300 ms

and 500 ms for EDL and SOL muscles respectively. Peak force (P_o) was recorded for each tetni, followed by an adjustment in muscle length. Once P_o had been established, no additional changes in the muscle length were made. Current was then increased until there was no further increase in P_o. Once L_o and supramaximal current had been established, additional isometric contractions were given every 3 minutes until the 1 hour time point of the experiment. At this point, L_o was measured, recorded, and the experimental protocol began.

Experimental Protocol

Each animal was randomly assigned to one of three bath treatments: Krebs-Ringer, Krebs-Ringer + DMSO, and Krebs-Ringer + DMSO + E-64-d. One muscle from the animal was subjected to an isometric contraction protocol and the contrallateral muscle to an eccentric protocol. Four EDL and 3 SOL muscles were studied per treatment for a total of 42 separate muscles.

Muscles performing the active eccentric contraction protocol performed one active isometric contraction at the beginning of the protocol in order to establish baseline force, 20 active eccentric contractions to induce muscle damage (67), and one final active isometric contraction to evaluate the loss of force due to damage. Muscles performing the active isometric protocol performed the exact same protocol as the active eccentric muscles except that the muscle was not lengthened. All contractions were separated by 3 minutes to give adequate time for recovery. Thus, the entire experimental protocol lasted 1 hour and 3 minutes.

During the eccentric protocol, muscles were lengthened by 20% of their initial fiber length (L_F) during the last 133 ms of stimulation. Thus the velocity of lengthening was 1.5 L_F/s. The magnitude of stretch was calculated from the L_o measurement and a published L_F to muscle length (L_M) ratio of 0.44 and 0.71 for EDL and SOL muscles respectively (12, 44). Upon completion of the last contraction, muscles were removed from the chambers, blotted dry, weighed, frozen in liquid nitrogen, and stored at -80°C until fodrin analysis was performed.

Muscle Homogenization

Muscles were pulverized under liquid nitrogen and suspended in ice-cold Tris-HCL buffer (20 mM Tris-HCl, 5 mM EDTA, 5 mM EGTA, 1 mM DTT, pH7.4) containing a broad spectrum protease inhibitor cocktail (Complete EGTA-Free Protease Inhibitor, Boehringer Mannheim, Indianapolis, IN). The protein homogenate was then centrifuged (10,000 rpm, 4°C) for 10 minutes and the supernatant assayed in triplicate for total protein concentration using the Bio-Rad RC DC Protein Assay Kit II (500-0122, Bio-Rad, Hercules, CA) on a 96-well microplate spectrophotometer.

Gel Electrophoresis

The solubilized protein samples were diluted to a concentration of 1 µg/µl with Tris-HCl buffer (20 mM Tris-HCl, 5 mM EDTA, 5 mM EGTA, 1 mM DTT, protease inhibitor cocktail, pH 7.4) and SDS loading buffer (1x SDS: 62.5 mM Tris pH 6.8, 2% SDS, 10% glycerol, 5% beta-mercaptoethanol, 0.001% bromophenl blue), and denatured (100°C) for 2-3 minutes. Samples were loaded onto a Bio-Rad Protean 3

minigel system (15 lanes per gel, 10 μg protein loaded per lane) consisting of a 3.5% stacking gel (3.5% acrylamide (2.7% bis), 0.125 M Tris (pH 6.8), 0.1% SDS, 0.045% APS, 0.15% TEMED) and a 6% separating gel (6% acrylamide (2.7% bis), 0.375 M Tris (pH 8.8), 0.1% SDS, 0.03% APS, 0.1% TEMED). Samples were electrophoresed for 75 minutes at a constant 200V at 4°C.

Western Blotting

Proteins were wet transferred overnight onto PVDF membranes (30V constant, 4°C) in a buffer consisting of 25mM Tris and 192 mM glycine. Blots were removed and blocked with 5% nonfat dry milk in a Tween-Tris buffered saline solution (TTBS: 50 mM tris-HCl, 150 mM NaCl, 0.05% Tween-20, pH 7.4). Blots were probed with mouse antispectrin monoclonal antibody (MAB1622, Chemicon, Temecula, CA) in TTBS (1:1000) at room temperature. Blots were washed in TTBS solution before being incubated in the secondary antibody, goat anti-mouse HRP conjugate (170-5040, Bio-Rad, Hercules, CA) in TTBS (1:2,000), at room temperature. Blots were washed in TTBS solution. Antigens were detected using the Immun-Star HRP chemiluminescent kit (170-5040, Bio-Rad, Hercules, CA) and the blots were imaged using a Flour-Chem gel imaging system (Alpha Innotech, San Leandro, CA). The amount of protein in each band of interest was quantified after background subtraction using ImageJ software (NIH, Bethesda, MD).

Statistical Analysis

Changes in the production of muscle force during the experimental protocol, as well as the analysis of the pixel density of the 150 and 145 kDa -fodrin fragment bands produced during the Western blotting procedures, were analyzed using a two-way ANOVA with main effects of bath treatment (Ringer-only, Ringer + DMSO, Ringer +DMSO + E-64-d) and contraction mode (isometric, eccentric). For muscle force, a repeated effect of time (pre, post) was included in the analysis. Significant main and interactive effects were further analyzed using Tukey's post hoc test. Statistical significance was set at $p<0.05$.

Results

Characteristics of EDL Muscles Prior to Treatment

Four EDL muscles were studied in each experimental condition. Muscle mass measurements (Table 1) were not significantly different between the experimental conditions, however, L_o measurements (Table 2) in the DMSO treatment condition were 7% shorter ($p<0.0006$) than in the Ringer-only and DMSO + E-64-d treatment condition groups. Because the eccentric treatment muscles were stretched at a relative percent of L_o, the small difference in L_o had no bearing on our results. Pre-treatment forces (Table 3) were also not significantly different between the experimental conditions.

Characteristics of SOL Muscles Prior to Treatment

Three SOL muscles were studied in each experimental condition. Both muscle mass (Table 4) and L_o measurements (Table 5) were not significantly different between the experimental conditions. Pre-treatment forces (Table 6) were also not significantly different between the experimental conditions. However, the slightly younger animals used in the DMSO group appears to be the cause of their slightly lower values.

Response of EDL Muscles to Isometric and Eccentric Contractions

Figure 1 shows representative force responses of EDL muscles to isometric and eccentric treatments. Force tracings, of muscles undergoing eccentric contractions, display an increase in P_o due to the lengthening protocol. Following the cessation of the stimulation phase, the motor lever arm remained in the lengthened position causing the muscle to remain in a lengthened state, producing the slight increase in baseline force. Force returned to baseline levels when the motor lever arm was returned back to L_o. Contractions numbered 1, 10, and 20 show a gradual decline in P_o for the eccentrically damaged muscles, whereas the P_o of the isometric muscles remained relatively stable.

Repeated measures analysis (Table 7) showed a significant time effect ($p<0.0001$) and a significant time by mode of contraction interaction ($p<0.0001$). Thus, the general mean of the muscles performing eccentric contractions differed from the general mean of the muscles performing isometric contractions as one moved from pre- to post-force measurements across time. These results were further examined by

analyzing the absolute and relative changes in pre- and post-forces for all experimental conditions (Table 8, Table 9).

On average, EDL force declined by 4% or 13 mN, across the 20 isometric contractions conducted in the Ringer-only solution (Table 8, Table 9). This was equivalent to an average change of 0.2% per contraction. Responses during the DMSO and DMSO + E-64-d trails were not significantly different from the Ringer-only trial, with average overall declines of 10% or 33 mN (0.5% per contraction) and 7% or 24 mN (0.3% per contraction) respectively.

EDL muscles undergoing eccentric contractions exhibited significantly greater overall declines in force ($p<0.0001$) compared to their respective isometric trials (Table 8, Table 9). For example, during the Ringer-only trial, overall force declined by 28% or 90mN. This was equivalent to an average change of around 1.4% per contraction, or five to six times greater than the response of the isometric Ringer-only trials. Responses during the DMSO and DMSO+E-64-d trails were similar to the Ringer-only trial, with overall declines of 21% or 72mN (1.1% per contraction) and 25% or 96mN (1.3% per contraction) respectively.

Response of SOL Muscles to Isometric and Eccentric Contractions

Figure 1 also shows representative force response of SOL muscles to isometric and eccentric treatments. Similar to the EDL muscles, contractions numbered 1, 10, and 20 show a gradual decline in P_o for the eccentrically damaged muscles, whereas the P_o of the isometric muscles remained relatively stable.

Repeated measures analysis (Table 10) showed a significant time effect ($p<0.0001$) and a significant time by bath treatment interaction ($p<0.05$). Unlike the EDL muscles, for the SOL muscles, one of the mean treatment responses differed from one or two of the other mean treatments as one moved from pre- to post-force. However, this is most likely due to the lower pre-treatment force of the DMSO trials. For SOL muscles, there was also a significant time by mode of contraction interaction ($p<0.0001$). As with the EDL, the general mean of the muscles performing eccentric contractions differed from the general mean of the muscles performing isometric contractions as one moved from pre- to post-force measurements across time. These results were also further examined by analyzing the absolute and relative changes in pre- and post-forces for all experimental conditions (Table 11, Table 12).

For muscles in the Ringer-only solution, force declined by 2% or 4mN (Table 11, Table 12), equivalent to an average change of 0.1% per contraction. Responses during the DMSO + E-64-d trails were not significantly different from the Ringer-only trials, with overall declines in force of 3.5% or 6 mN (0.2% per contraction). Absolute force losses (0.5 mN, Table 11) were significantly ($p<0.05$) less for the DMSO trials. However, this appeared to be due in part to the slightly lower pre-treatment force of the DMSO trials (Table 6) because, when expressed as a percent change (Table 12), no differences were observed in force loss for each treatment.

SOL muscles undergoing eccentric contractions exhibited significantly greater overall declines in force ($p<0.0001$) compared to their respective isometric trials (Table 11, Table 12). Force declined by 28% or 54mN for SOL muscles in the Ringer-only trial. This decline is equivalent to a change of around 1.4% per

contraction. Responses during the DMSO and DMSO + E-64-d trails were also very similar to the Ringer-only trial, with overall declines in force of 23% or 34mN (1.1% per contraction) and 23% or 47mN (1.2% per contraction) respectively. Thus, changes in P_o following the eccentric protocol are around seven to eight times greater than the changes observed for the isometric protocol.

α-Fodrin Proteolysis of EDL Muscles

EDL muscle homogenates were analyzed by Western blotting to determine the extent of α-fodrin fragment production. For the EDL muscles, individual gels were run for each bath treatment. To facilitate comparisons between gels, a muscle standard was run on each gel. These standards were prepared from EDL and gastrocnemius muscles processed exactly as outlined in the Methods section for the experimental muscle samples. Individual EDL muscles were homogenized for individual muscle standards, whereas several gastrocnemius muscles were combined to form one gastrocnemius muscle standard. All muscles used for standards were dissected and immediately frozen for homogenization.

Figures 2 through 4 clearly display the presence of both an intact α-fodrin band at 280 kDa, as well as separate 150 and 145 kDa α-fodrin fragment bands in all muscle samples. Visual analysis of the figures displays a decrease in the levels of 150 and 145 kDa α-fodrin fragments for muscles in the bath containing DMSO + E-64-d.

ImageJ software was used to determine the raw pixel density after background subtraction of both the intact α-fodrin band (Table 13) and the 150 and 145 kDa α-fodrin fragment bands for each muscle sample. The two values of the 150 and 145

kDa α-fodrin fragment bands were combined into one final value for each muscle sample and were recorded as a raw pixel density value (Table 14). In addition, a normalized value based off the muscle standard samples was calculated (Table 15). Because each gel was loaded with identical muscle standards and varying experimental muscles, normalized values were calculated by expressing the 150 and 145 kDa α-fodrin fragments as a percentage of the 150 and 145 kDa α-fodrin fragments of the muscle standards on each gel.

A two-way ANOVA with main effects of bath treatment and contraction type with Tukey's post hoc analysis revealed no significant difference in the integrated density of the intact (280 kDa) α-fodrin bands for all experimental conditions (Table 13). A significant difference ($p<0.003$) between the DMSO + E-64-d bath treatment, compared to the other bath treatments, was observed for the 150 and 145 kDa α-fodrin bands regardless of whether data were analyzed as raw values (Table 14) or normalized to our muscle standard (Table 15). Thus, E-64-d treatment reduced α-fodrin breakdown in both isometric and eccentric treatments. However, there was no mode of contraction difference in α-fodrin breakdown for either the raw or normalized data.

α-Fodrin Proteolysis of SOL Muscles

SOL muscle homogenates were analyzed by Western blots exactly as detailed above for the EDL muscles. Two gels were run for the SOL muscles, one containing the Ringer-only and DMSO+E-64-d muscle homogenates and another with the DMSO

muscle homogenates. The muscle standards used on these gels were prepared from SOL and gastrocnemius muscles.

Similar to the EDL muscles, Figures 5 and 6 clearly display the presence of intact and fragment α-fodrin bands. ImageJ software was used to determine raw pixel density values as outlined above (Table 16, Table 17, Table 18).

A two-way ANOVA with main effects of bath treatment and contraction type with Tukey's post hoc analysis displayed a significant difference ($p<0.009$) between the intact α-fodrin levels of the isometric and eccentric muscles with the isometric band having around 40% more intact α-fodrin. As with the EDL muscles, the results displayed significant differences ($p<0.0002$) between the raw and normalized 150 and 145 kDa α-fodrin fragments of the DMSO+E-64-d compared to the other bath treatments. Thus, as with the EDL muscles, E-64-d treatment reduced α-fodrin breakdown in both isometric and eccentric treatments. However, there was no mode of contraction difference in α-fodrin breakdown for either the raw or normalized data.

Table 1.
Muscle Mass of EDL Muscles

	Ringer	DMSO	E-64-d	mean
isometric	9.8 ± 0.6	9.5 ± 0.7	10.0 ± 0.3	9.8 ± 0.3
eccentric	9.6 ± 0.2	9.6 ± 0.6	10.2 ± 0.6	9.8 ± 0.3
mean	9.7 ± 0.3	9.5 ± 0.4	10.1 ± 0.3	

Values are means ± SE with n = 4 muscles for each experimental condition. Abbreviations: Ringer, Ringer-only; DMSO, Ringer plus dimethyl sulfoxide; E-64-d, Ringer plus dimethyl sulfoxide plus E-64-d.

Table 2.
L_o of EDL Muscles

	Ringer	DMSO	E-64-d	mean
isometric	12.8 ± 0.2	11.8 ± 0.1	12.6 ± 0.2	12.4 ± 0.2
eccentric	12.9 ± 0.1	12.2 ± 0.3	12.9 ± 0.3	12.6 ± 0.2
mean	12.9 ± 0.1	11.9 ± 0.2 *	12.8 ± 0.2	

Values are means ± SE with n = 4 muscles for each experimental condition. * indicates significant DMSO treatment effect, $p<0.0006$. Abbreviations same as Table 1.

Table 3.
Pre-Treatment Force (kN/m^2) of EDL Muscles

	Ringer	DMSO	E-64-d	mean
isometric	192 ± 21	191 ± 16	206 ± 25	196 ± 20
eccentric	200 ± 18	199 ± 19	222 ± 16	183 ± 23
mean	196 ± 7	195 ± 6	214 ± 8	

Values are means ± SE with n = 4 muscles for each experimental condition.
Abbreviations same as Table 1.

Table 4.
Muscle Mass of SOL Muscles

	Ringer	DMSO	E-64-d	mean
isometric	7.7 ± 0.6	7.6 ± 0.2	8.3 ± 0.6	7.9 ± 0.3
eccentric	7.8 ± 0.6	7.3 ± 0.3	8.2 ± 0.3	7.8 ± 0.2
mean	7.8 ± 0.4	7.4 ± 0.2	8.3 ± 0.3	

Values are means ± SE with n = 3 muscles for each experimental condition.
Abbreviations same as Table 1.

Table 5.
L_o of SOL Muscles

	Ringer	DMSO	E-64-d	mean
isometric	10.9 ± 0.2	11.6 ± 0.3	11.9 ± 0.2	11.5 ± 0.2
eccentric	11.7 ± 0.3	11.6 ± 0.4	11.8 ± 0.4	11.7 ± 0.2
mean	11.3 ± 0.2	11.6 ± 0.2	11.9 ± 0.2	

Values are means ± SE with n = 3 muscles for each experimental condition.
Abbreviations same as Table 1.

Table 6.
Pre-Treatment Force (kN/m^2) of SOL Muscles

	Ringer	DMSO	E-64-d	mean
isometric	196 ± 18	201 ± 4	198 ± 33	198 ± 19
eccentric	218 ± 14	180 ± 18	223 ± 12	207 ± 24
mean	207 ± 8	190 ± 7	210 ± 7	

Values are means ± SE with n = 3 muscles for each experimental condition.
Abbreviations same as Table 1.

Table 7.
Pre and Post-Treatment Force of EDL Muscles (mN)

		Ringer	DMSO	E-64-d	mean
isometric	pre	313 ± 30	327 ± 28	351 ± 57	330 ± 40
	post	299 ± 26	294 ± 31	328 ± 56	307 ± 40
		306 ± 28	311 ± 30	340 ± 57	319 ± 40
eccentric	pre	317 ± 37	337 ± 37	375 ± 33	343 ± 41
	post	226 ± 20	265 ± 26	279 ± 16	257 ± 30 *
		272 ± 29	301 ± 32	327 ± 25	300 ± 36

Values are means ± SE with n = 4 muscles for each experimental condition.
* indicates significant eccentric treatment effect, $p<0.0001$. Abbreviations same as Table 1.

Table 8.
Change in Force (mN) as a Result of the
Isometric or Eccentric Treatments for EDL Muscles.

	Ringer	DMSO	E-64-d	mean
isometric	13.3 ± 3.3	32.9 ± 11.8	23.8 ± 5.7	23.6 ± 4.7
eccentric	90.8 ± 9.8	72.0 ± 8.2	95.9 ± 9.6	86.2 ± 5.7 *
mean	52.1 ± 15.4	52.5 ± 10.0	59.8 ± 14.6	

Values are means ± SE with n = 4 muscles for each experimental condition.
* indicates significant eccentric treatment effect, $p<0.0001$. Abbreviations same as Table 1.

Table 9.
Percent Change in Force as a Result of the
Isometric or Eccentric Treatments for EDL Muscles.

	Ringer	DMSO	E-64-d	mean
isometric	4.2 ± 0.9	10.0 ± 3.5	6.8 ± 1.5	7.0 ± 1.4
eccentric	28.4 ± 1.5	21.3 ± 1.8	25.4 ± 1.6	25.0 ± 1.2 *
mean	16.3 ± 4.7	15.6 ± 2.8	16.1 ± 3.6	

Values are means ± SE with n = 4 muscles for each experimental condition.
* indicates significant eccentric treatment effect, $p<0.0001$. Abbreviations same as Table 1.

Table 10.
Pre and Post-Treatment Forces of SOL Muscles (mN)

		Ringer	DMSO	E-64-d	mean
isometric	pre	186 ± 36	175 ± 14	184 ± 31	182 ± 25
	post	183 ± 33	174 ± 13	178 ± 32	178 ± 24
		185 ± 35	175 ± 14	181 ± 32	180 ± 25
eccentric	pre	195 ± 34	151 ± 19	206 ± 20	184 ± 33
	post	140 ± 33	116 ± 18	158 ± 22	138 ± 28 *
		168 ± 34	133 ± 19	182 ± 21	161 ± 31

Values are means ± SE with n = 3 muscles for each experimental condition.
* indicates significant eccentric treatment effect, $p<0.0001$. Abbreviations same as Table 1.

Table 11.
Change in Force (mN) as a Result of the
Isometric or Eccentric Treatments for SOL Muscles.

	Ringer	DMSO	E-64-d	mean
isometric	3.6 ± 2.0	0.5 ± 1.0	6.2 ± 2.1	3.4 ± 1.2
eccentric	54.3 ± 7.0	34.1 ± 6.7	47.4 ± 1.8	45.2 ± 4.1 *
mean	28.9 ± 11.8	17.3 ± 8.1 *	26.8 ± 9.3	

Values are means ± SE with n = 3 muscles for each experimental condition.
* indicates significant eccentric treatment effect, $p<0.0001$; as well as significant DMSO treatment effect $p<0.05$. Abbreviations same as Table 1.

Table 12.
Percent Change in Force as a Result of the
Isometric or Eccentric Treatments for SOL Muscles.

	Ringer	DMSO	E-64-d	mean
isometric	1.7 ± 0.9	0.2 ± 0.6	3.5 ± 1.2	1.8 ± 0.7
eccentric	28.2 ± 4.0	22.7 ± 4.1	23.2 ± 2.0	24.7 ± 1.9 *
mean	14.9 ± 6.2	11.5 ± 5.3	13.4 ± 4.5	

Values are means ± SE with n = 3 muscles for each experimental condition.
* indicates significant eccentric treatment effect, $p<0.0001$. Abbreviations same as Table 1.

Table 13.
Integrated Density of Intact α-Fodrin
From EDL Muscles

	Ringer	DMSO	E-64-d	mean
isometric	0.013 ± 0.003	0.01 ± 0.001	0.009 ± 0.001	0.011 ± 0.001
eccentric	0.009 ± 0.001	0.01 ± 0.001	0.006 ± 0.001	0.008 ± 0.001
mean	0.011 ± 0.002	0.01 ± 0.001	0.008 ± 0.001	

Values are means ± SE with n = 4 muscles for each experimental condition. Abbreviations same as Table 1.

Table 14.
Integrated Density of 150 and 145 kDa α-Fodrin Fragments
From EDL Muscles

	Ringer	DMSO	E-64-d	mean
isometric	0.012 ± 0.003	0.011 ± 0.001	0.004 ± 0.001	0.009 ± 0.001
eccentric	0.008 ± 0.001	0.009 ± 0.001	0.004 ± 0.000	0.007 ± 0.001
mean	0.01 ± 0.001	0.01 ± 0.001	0.004 ± 0.000 *	

Values are means ± SE with n = 4 muscles for each experimental condition. * indicates significant E-64-d treatment effect, $p<0.003$. Abbreviations same as Table 1.

Table 15.
Normalized Integrated Density of α-Fodrin Fragments
From EDL Muscles

	Ringer	DMSO	E-64-d	mean
isometric	4.5 ± 1.3	4.2 ± 0.3	2.0 ± 0.3	3.6 ± 0.5
eccentric	3.1 ± 0.4	3.5 ± 0.4	1.7 ± 0.2	2.8 ± 0.3
mean	3.8 ± 0.7	3.9 ± 0.3	1.8 ± 0.2 *	

Values are means ± SE with n = 4 muscles for each experimental condition. Values were normalized by dividing each muscle sample's 150 &145 kDa integrated density value by the 150 & 145 kDa integrated density value of the muscle standard loaded on that gel. Each gel was loaded with identical muscle standards. * indicates significant E-64-d treatment effect, $p<0.006$. Abbreviations same as Table 1.

Table 16.
Integrated Density of Intact α-Fodrin
from SOL Muscles

	Ringer	DMSO	E-64-d	mean
isometric	0.022 ± 0.003	0.023 ± 0.005	0.015 ± 0.003	0.020 ± 0.033
eccentric	0.013 ± 0.005	0.013 ± 0.002	0.007 ± 0.001	0.011 ± 0.002 *
mean	0.017 ± 0.003	0.018 ± 0.003	0.011 ± 0.002	

Values are means ± SE with n = 3 muscles for each experimental condition. * indicates significant isometric treatment effect, $p<0.009$. Abbreviations same as Table 1.

Table 17.
Integrated Density of 150 and 145 kDa α-Fodrin Fragments
from SOL Muscles

	Ringer	DMSO	E-64-d	mean
isometric	0.022 ± 0.003	0.018 ± 0.002	0.007 ± 0.001	0.016 ± 0.002
eccentric	0.014 ± 0.004	0.018 ± 0.005	0.004 ± 0.001	0.012 ± 0.003
mean	0.018 ± 0.003	0.018 ± 0.002	0.006 ± 0.001 *	

Values are means ± SE with n = 3 muscles for each experimental condition. * indicates significant E-64-d treatment effect, $p<0.002$. Abbreviations same as Table 1.

Table 18.
Normalized Integrated Density of α-Fodrin Fragments
from SOL Muscles

	Ringer	DMSO	E-64-d	mean
isometric	0.72 ± 0.08	0.69 ± 0.06	0.24 ± 0.03	0.55 ± 0.08
eccentric	0.45 ± 0.15	0.66 ± 0.18	0.14 ± 0.03	0.42 ± 0.10
mean	0.59 ± 0.10	0.68 ± 0.09	0.19 ± 0.03 *	

Values are means ± SE with n = 3 muscles for each experimental condition. Values were normalized by dividing each muscle sample's 150 &145 kDa integrated density value by the 150 & 145 kDa integrated density value of the muscle standard loaded on that gel. Each gel was loaded with identical muscle standards. * indicates significant E-64-d treatment effect, $p<0.002$. Abbreviations same as Table 1.

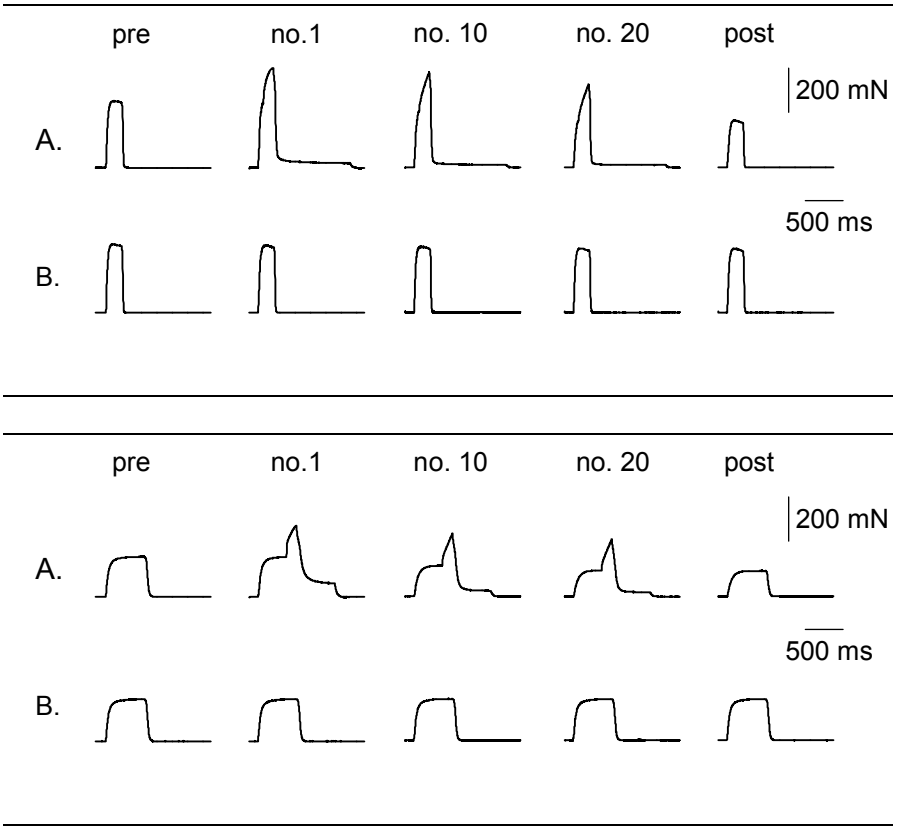

Figure 1. Force records obtained during each treatment. *top*, force records of EDL muscles performing eccentric contractions (row A) and isometric contractions (row B); *bottom*, force records of SOL muscles performing eccentric contractions (row A) and isometric contractions (row B). For brevity, only the pre and post isometric and the 1st, 10th, and 20th treatment contractions are shown.

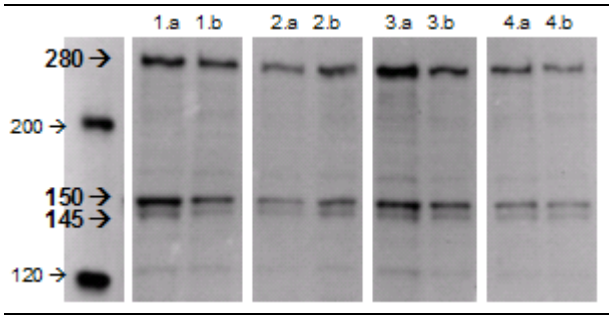

Figure 2. Western blots of α-fodrin in EDL muscles subjected to isometric and eccentric contractions in Krebs-Ringer. The numbers 1-4 indicate animal; the letters *a & b* indicate contraction type, isometric or eccentric respectively.

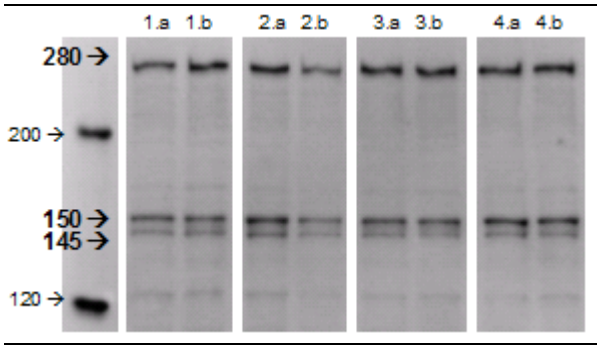

Figure 3. Western blots of α-fodrin in EDL muscles subjected to isometric and eccentric contractions in Krebs-Ringer + DMSO. The numbers 1-4 indicate animal; the letters *a & b* indicate contraction type, isometric or eccentric respectively.

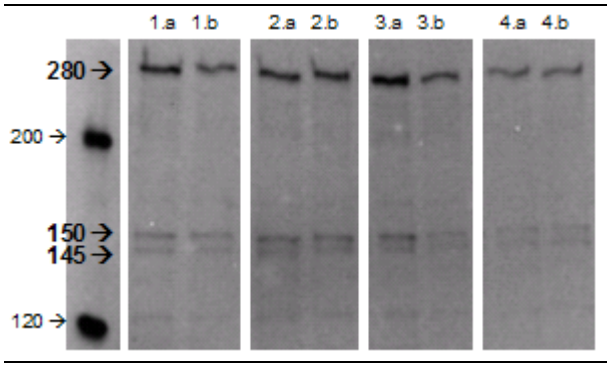

Figure 4. Western blots of α-fodrin in EDL muscles subjected to isometric and eccentric contractions in Krebs-Ringer + DMSO + E-64-d. The numbers 1-4 indicate animal; the letters *a & b* indicate contraction type, isometric or eccentric respectively.

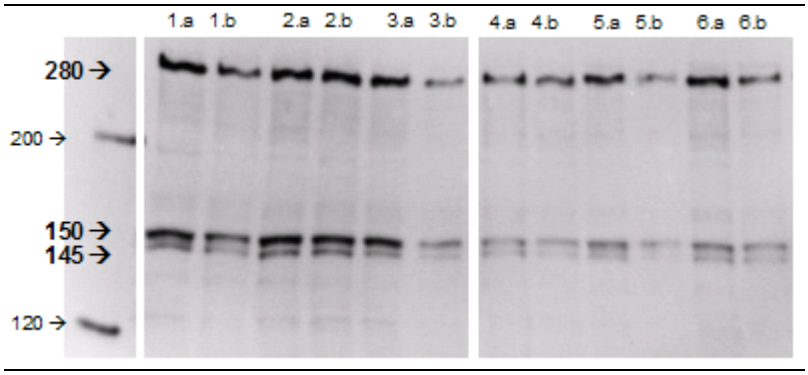

Figure 5. Western blots of α-fodrin in SOL muscles subjected to isometric and eccentric contractions in Krebs-Ringer (1-3) and Krebs-Ringer + DMSO + E64-d (4-6). The numbers 1-6 indicate animal; the letters *a & b* indicate contraction type, isometric or eccentric respectively.

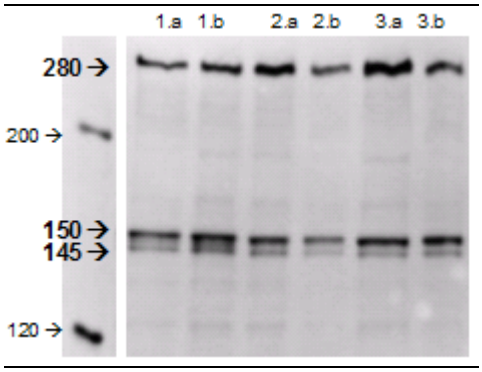

Figure 6. Western blots of α-fodrin in SOL muscles subjected to isometric and eccentric contractions in Krebs-Ringer + DMSO + E-64-d. The numbers 1-3 indicate animal; the letters *a & b* indicate contraction type, isometric or eccentric respectively.

Discussion

Relevance of Study

Calpains, or Ca^{2+}-activated neutral proteases, have been implicated in the process of muscle proteolysis (22, 29, 52, 55). Specifically, calpains have been proposed to target proteins located in the Z-band region, causing the loss of myofibrillar alignment and initiating destruction of the myofibril. It has been hypothesized that perhaps an exercise-induced activation of calpains occurs and is responsible for the associated damage.

Loss of A-band register, Z-band streaming, and accelerated protein degradation are all characteristics of muscles injured by eccentric contractions (13, 37, 45, 67, 74). Furthermore, muscles damaged in this way show elevated $[Ca^{2+}]_i$ at rest (43). Thus, it has been proposed that calpains are activated after exercise-induced muscle damage and are responsible for the initial protein degradation and disassembly of the muscle (9, 10). While this is an attractive theory, it has never been rigorously tested under *in vitro* conditions present in damaged muscle cells. The purpose of the present study was to test the hypothesis that calpains are activated *in vivo* following a series of eccentric contractions.

To accomplish these goals, we subjected mouse EDL and SOL muscles to an eccentric or isometric protocol under one of three bath treatments: Krebs-Ringer, Krebs-Ringer + DMSO, Krebs-Ringer + DMSO + the cysteine protease inhibitor E-64-d. Following the contractile treatments, each muscle was analyzed via Western

blots to determine the breakdown of the intact 280 kDa α-fodrin protein into 150 and 145 kDa α-fodrin fragments. The appearance of 150 and 145 kDa α-fodrin fragments is a highly sensitive and widely accepted marker of *in vivo* calpain proteolysis (22, 29, 62, 75). This approach has been used previously for measuring calpain activity in cultured muscle cells (29) and in models of cardiac dysfunction (62, 75). Here we have applied this approach to evaluate calpain activity in skeletal muscles after exercise-induced damage.

Care was taken to use experimental treatments that were physiologically relevant. First, we examined both glycolytic (EDL) and oxidative (SOL) muscles. Studies looking at the interaction between muscle damage and muscle fiber type have displayed an increased susceptibility of type II muscle fibers to damage (17, 19, 20, 35, 73). In the ICR strain of mice, EDL muscles are composed of type IIx and IIb (fast) fibers (1), whereas SOL muscles have relatively equal distribution of type I (slow) and type IIa (fast) fibers (58).

Second, the extent of muscle damage is highly dependent on the magnitude of the stretch applied to the muscle. Our lengthening protocol stretched muscles by 20% of their L_F. This is well within the physiological range of sarcomere length excursion, which for biarticulate muscles, can reach over 50% of L_F (13).

Third, we also believed that is was important to study the muscles at a physiological temperature. Muscles studied between 30 and 37°C show a greater accumulation of $[Ca^{2+}]_i$ versus muscles which are studied at temperatures < 30°C (70). Because our model predicts calpain activation as $[Ca^{2+}]_i$ levels rise, experiments

conducted at a lower temperatures may exhibit altered $[Ca^{2+}]_i$ levels and calpain responses than those conducted at a physiological temperature.

Main Findings

The main findings of this study are as follows. First, muscles performing the eccentric protocol showed a greater overall reduction in P_o compared to muscles performing the isometric protocol. Second, the use of the calpain inhibitor E-64-d served to decrease the levels of 150 and 145 kDa α-fodrin fragments observed in the muscles, regardless of the contraction protocol. Third, there was no evidence that eccentric muscle damage increased the levels of 150 and 145kDa α-fodrin fragments over the levels observed in the isometric trials. Thus, even though muscles were damaged by the protocol, and the E-64-d concentration used was sufficient to inhibit calpain activity, there was no difference in our marker of calpain activity in control or damaged muscles. Based on these observations, we reject our original hypothesis. Thus, under the present experimental conditions, eccentric exercise did not increase calpain activity, at least as revealed by analysis of α-fodrin degradation.

Relationship to Previous Work

Previous studies inducing muscle damage have subjected skeletal muscles to varying eccentric protocols. These protocols have varied from a single stretch to as many as 900 eccentric contractions. In our study we subjected EDL and SOL muscles to 20 eccentric or isometric contractions. We found that P_o dropped 21-28% and 22-28% in eccentrically damaged EDL and SOL muscles respectively. Conversely, EDL

and SOL muscles subjected to non-damaging isometric contractions maintained a fairly constant force throughout the protocol in that force dropped only 4-10% and 1-4% for EDL and SOL muscles respectively.

Several studies involving mouse EDL and SOL muscles performing isometric contractions, studied at 37 °C *in vitro*, have displayed similar findings to our results. The first study subjected SOL muscles to 20 isometric contractions and found that P_o dropped by only 4% (72). Another study involving both EDL and SOL muscles found that after 15 isometric contractions P_o declined by 15% and 1% respectively (69). Thus our isometric protocol is in agreement with other isometric findings.

However, for studies involving eccentric contractions, the results are varied. In a study subjecting SOL muscles to stretches of 25% of L_o, P_o declined by 42% after 20 eccentric contractions (72). In another study involving EDL and SOL muscles, muscles were stretched at 10% of L_o which caused P_o to drop by 61% and 8% respectively after 15 eccentric contractions (69). The discrepancies with our results appear to be due to the difference in the magnitude of stretch applied to the muscles. Our 20% of L_F is different than 10% or 25% of L_o. Assuming a L_F to L_M of 0.44 for EDL muscles, a stretch of 10% of L_o is approximately three times that of our stretch and a stretch of 25% of L_o is six times that of ours. However, because the L_F to L_M ratio of SOL muscles is 0.71, the disparity is not quite as large. A stretch of 10% of L_o is actually very similar to that of our protocol and a stretch of 25% of L_o is three times that used in our study. Thus our eccentric protocol did not elicit the same degree of damage as in other eccentric findings, most likely due to the differences in the magnitude of stretch.

Regardless of the actual percentage, all of these studies with eccentrically damage muscles show a gradual yet steady decline in P_o across the duration of the protocol, compared to the relatively minimal decline of the isomeric muscles (41, 69, 72). This suggests that the observed drop in P_o found in our study is congruent with the magnitude of stretch associated with our protocol.

Novel Observations from the Present Work

One of the aims of this study was to determine whether the use of E-64-d would cause a reduction in the amount of α-fodrin breakdown after damaging muscle contractions. Previous studies have used injections of E-64-d to inhibit calpain activity *in vivo* in spinal cord injury and muscular dystrophy models (38, 49, 50). We were interested in the ability to use a calpain inhibitor as a way of examining calpain mediated proteolysis in a model of exercise-induced muscle damage. We used an *in vitro* preparation because this preparation will allow the manipulation of other variables of interest, such as $[Ca^{2+}]_o$ concentration in future studies.

One previous study used E-64-d in an *in vitro* preparation with muscles subjected to eccentric contractions (70). However, this study made no evaluation as to whether the inhibitor was able to enter the muscle and inhibit protein breakdown. Thus, to our knowledge, the present project is the first to examine the effectiveness of E-64-d in reducing α-fodrin breakdown in an isolated muscle studied *in vitro*. Our findings indicate that the E-64-d concentration used and the duration of incubation were sufficient to reduce α-fodrin breakdown into 150 and 145 kDa fragments in isolated EDL and SOL muscles. Because the appearance of these α-fodrin positive

fragments is a well accepted marker of calpain activation, our results suggest that our E-64-d treatment was able to inhibit calpain activation. This is a critical finding for future studies.

E-64-d must be dissolved in an organic solvent. Thus, another important finding of this study is that the vehicle used to dissolve the E-64-d, DMSO, when used at our concentrations, had no effect on any of the variables examined.

Based on our model of exercise-induced muscle damage, we expected to see greater levels of 150 and 145kDa α-fodrin fragments in those muscles that performed the eccentric protocol versus those that performed the isometric protocol. However, Western blot analysis displayed similar levels of α-fodrin breakdown in muscles performing eccentric and isometric protocols. This observation held for both EDL and SOL muscles. Thus, we reject our hypothesis that calpains are activated in muscles damaged by eccentric muscle contractions.

Limitations and Future Directions

Contrary to our hypothesis, our Western blot analysis did not display an increased α-fodrin breakdown for muscles performing eccentric contractions versus isometric contractions. One possible explanation is that the eccentric protocol activated calpains but there are complications in the analysis of that activity. There may be the potential for a time-dependency of the breakdown of the 150 and 145 kDa α-fodrin fragments. For example, in the study by Yoshida (75) looking at the degradation of α-fodrin in damaged heart muscle, the amount of the intact α-subunit, as seen by Western blotting, gradually decreased as the length of the experimental

protocol increased up to the maximum of sixty minutes. Concurrently, there was an increase in the amount of 150 kDa α-fodrin fragment formation. Of particular interest is the finding that this increase in the 150 kDa α-fodrin fragment formation peaked around twenty minutes, at which time the level of 150 kDa α-fodrin fragment formation actually began to decline. Our interpretation of this data is that there had been an increased amount of α-fodrin breakdown over the 60 minute experiment. With increased breakdown of intact α-fodrin, there is most likely an increase in the breakdown of the subsequent 150 and 145 kDa α-fodrin fragments. If these 150 and 145 kDa α-fodrin fragments are broken into even smaller subunits, a measurement of the production of these 150 and 145 kDa α-fodrin fragments at an unspecified time point might lead to inaccurate measurements in the actual amount of damage which has occurred. Thus, we may have misinterpreted our α-fodrin results due to time-dependent degradation of the 150 and 145 kDa α-fodrin fragments.

An alternative explanation deals with whether EDL and SOL muscles placed in a Krebs-Ringer bath receive adequate oxygen levels when they are stimulated. Because the muscles have been dissected from the animals, all nutrients are received through diffusion. It is possible that during the experiment, the muscles are hypoxic, with calpains potentially being very sensitive to even the slightest degree of hypoxia. A study looking at the physiological performance of cardiac muscle at varying temperatures (27.5-37.5° C) and frequencies (1-8 Hz) displayed that contractile performance was diminished in those muscles with a diameter of > 0.15 mm (48). Although the diameters of the muscles used in our study were not measured, their P_o

values held up very well through the experimental protocol. This argues against the idea that the preparation adversely influenced the muscles performance.

Another possible explanation for our findings is that α-fodrin breakdown doesn't occur during lengthening contractions. This particular explanation does not appear to be likely based upon the following. Electron microscopy of eccentrically damaged muscles shows the disorganization of myofibrils with entire regions of myofibrils within the sarcomere out of alignment with each other (7). The disrupted striation patterns display actin filament displacement from myosin filaments as well as the loss of visually distinguishable sarcomeres and Z-bands (13, 67, 74). In contrast, fibers from isometrically contracted muscles contain sarcomeres of normal appearance, organized in a regular array, and aligned with sarcomeres of neighboring myofibrils (7). These alterations in eccentrically contracted muscles indicate possible loss of contractile and series elements, such as the Z-band (13, 67, 74), of which α-fodrin is a component.

In the heart studies where there was induced contractile dysfunction, distinct differences in the amount of α-fodrin breakdown were noticeable between damaged and non-damaged heart tissue (62, 75). However this difference was not apparent between our damaged muscles. Both the damaged and non-damaged muscles displayed similar α-fodrin breakdown levels. The most logical explanation for this is simply that the damage associated with our eccentric protocol was not of significant magnitude to induce calpain activation. Thus, the levels of α-fodrin breakdown between the eccentric and isometric muscles are similar. While we cannot confirm

this idea, the possibility that calpain activation is sensitive to the amount or degree of damage should be pursued in future studies.

Conclusion

It was hypothesized that calpains are involved in the process of muscle damage. In order to test this hypothesis, we subjected muscles to damaging protocols both with and without a calpain inhibitor. Our results indicate that the inhibitor used, E-64-d, could reduce calpain activity, as assessed by the appearance of 150 and 145 kDa α-fodrin positive peptides, *in vitro*. However, we found no difference in α-fodrin breakdown between muscles subjected to eccentric and isometric treatments. In fact, there appeared to be little increase in α-fodrin degradation as a result of either contractile treatment. This suggests that the magnitude of damage was insufficient to activate calpains. Future studies looking at the effect of the magnitude of injury will help to further determine the role that calpains may play in muscle damage.

Bibliography

1. **Agbulut O, Li Z, Mouly V, and S B-BG.** Analysis of skeletal and cardiac muscle from desmin knock-out and normal mice by high resolution separation of myosin heavy-chain isoforms. *Biology of the Cell* 88: 131-135, 1996.

2. **Allen DG, Whitehead NP, and Yeung EW.** Mechanisms of stretch-induced muscle damage in normal and dystrophic muscle: role of ionic changes. *Journal of Physiology* 567: 723-735, 2005.
3. **Armstrong RB, Warren GL, and Warren JA.** Mechanisms of exercise-induced muscle fibre injury. *Sports Medicine* 12: 184-207, 1991.
4. **Au Y.** The muscle ultrastructure: a structural perspective of the sarcomere. *Cellular and Molecular Life Sciences* 61: 3016-3033, 2004.
5. **Badalamente MA and Stracher A.** Delay of muscle degeneration and necrosis in mdx mice by calpain inhibition. *Muscle Nerve* 23: 106-111, 2000.
6. **Balnave CD and Allen DG.** Intracellular calcium and force in single mouse muscle fibers following repeated contractions with stretch. *Journal of Physiology* 488: 25-36, 1995.
7. **Balnave CD, Davey DF, and Allen DG.** Distribution of sarcomere length and intracellular calcium in mouse skeletal muscle following stretch-induced injury. *Journal of Physiology* 502: 649-659, 1997.
8. **Barta J, Tóth A, Édes I, Vaszily M, Papp JG, Varró A, and Papp Z.** Calpain-1-sensitive myofibrillar proteins of the human myocardium. *Molecular and Cellular Biochemistry* 278: 1-8, 2005.
9. **Belcastro AN.** Skeletal muscle calcium-activated neutral protease (calpain) with exercise. *Journal of Applied Physiology* 74: 1381-1386, 1993.
10. **Belcastro AN, Shewchuk LD, and Raj DA.** Exercise-induced muscle injury: A calpain hypothesis. *Molecular and Cellular Biochemistry* 179: 135-145, 1998.
11. **Bodensteiner JB and Engel AG.** Intracellular calcium accumulation in Duchenne muscular dystrophy and other myopathes: a study of 567,000 muscle fibers in 114 biopsies. *Neurology* 28: 439-446, 1978.
12. **Brooks SV and Faulkner JA.** Contractile properties of skeletal muscles from young, adult and aged mice. *Journal of Physiology* 404: 71-82, 1988.
13. **Brooks SV, Zerba E, and Faulkner JA.** Injury to muscles after single stretches of passive and maximally stimulated muscles in mice. *Journal of Physiology* 488: 459-469, 1995.
14. **Carpenter S and Karpati G.** Duchenne muscular dystrophy: plasma membrane loss initiated muscle cell necrosis unless it is repaired. *Brain* 102: 147-161, 1979.
15. **Clarckson PM and Sayers SP.** Etiology of exercise-induced muscle damage. *Canadian Journal of Applied Physiology* 24: 234-248, 1999.
16. **Duan C, Delp MD, Hayes DA, Delp PD, and Armstrong RB.** Rat skeletal muscle mitochondrial [Ca^{2+}] and injury from downhill walking. *Journal of Applied Physiology* 68: 1241-1251, 1990.
17. **Edgerton VR, Zhou MY, Ohira Y, Klitgaard H, Jiang B, Bell G, Harris B, Saltin B, Gollnick PD, and Roy RR.** Human Fiber size and enzymatic properties after 5 and 11 days of spaceflight. *Journal of Applied Physiology* 78: 1733-1739, 1995.
18. **Féasson L, Stockholm D, Freyssenet D, Richard D, Duguez S, Beckmann JS, and Denis C.** Molecular adaptations of neuromuscular disease-associated proteins

in response to eccentric exercise in human skeletal muscle. *Journal of Physiology* 543: 297-306, 2002.
19. **Fitts RH, Riley DR, and Widrick JJ.** Functional and structural adaptations of skeletal muscle to microgravity. *Journal of Experimental Biology* 204: 3201-3208, 2001.
20. **Fitts RH, Riley DR, and Widrick JJ.** Physiology of a microgravity environment invited review: microgravity and skeletal muscle. *Journal of Applied Physiology* 89: 823-839, 2000.
21. **Fridén J and Lieber RL.** Eccentric exercise-induced injuries to contractile and cytoskeletal muscle fibre components. *ACTA Physiologica Scandivavica* 171: 321-326, 2001.
22. **Goll DE, Thompson VF, Li H, Wei W, and Cong J.** The calpain system. *Physiological Review* 83: 731-801, 2003.
23. **Goll DE, Thompson VF, Taylor RG, and Zalewska T.** Is calpain activity regulated by membranes and autolysis or by calcium and calpastatin? *BioEssays* 14: 549-556, 1992.
24. **Gordon AM, Huxley AF, and Julian FJ.** The variation in isometric tension with sarcomere length in vertebrate muscle fibers. *Journal of Physiology* 184: 170-192, 1966.
25. **Gordon AM, Huxley AF, and Julian FJ.** The variation in isometric tension with sarcomere length in vertebrate muscle fibers. *Journal of Physiology* 184: 170-192, 1966.
26. **Hoffman EP, Brown RH, and Kunkel LM.** Dystrophin, the protein product of the Duchenne muscular dystrophy locus. *Cell* 51: 919-928, 1987.
27. **Horowits R, Kemper ES, Bisher ME, and Podolsky RJ.** A physiological role for titin and nebulin in skeletal muscle. *Nature* 323: 160-164, 1986.
28. **Horowits R and Podolsky RJ.** The positional stability of thick filaments in activated skeletal muscle depends on sarcomere length: evidence for the role of titin filaments. *Journal of Cell Biology* 105: 2217-2223, 1987.
29. **Huang J and Forsberg NE.** Role of calpain in skeletal-muscle protein degradation. *Proceedings from the National Academy of Sciences* 95: 12100-12105, 1998.
30. **Huxley AF and Niedergerke R.** Structural changes in muscle during contraction. Inference microscopy of living muscle fibers. *Nature* 173: 971-973, 1954.
31. **Huxley HE.** Fifty years of muscle and the sliding filament hypothesis. *European Journal of Biochemistry* 271: 1403-1415, 2004.
32. **Huxley HE and Hanson J.** Changes in the cross-striations of muscle during contraction and stretch and their structural interpretation. *Nature* 173: 973-976, 1954.
33. **Ingalls CP, Warren GL, Williams JH, Ward CW, and Armstrong RB.** E-C coupling failure in mouse EDL muscle after in vivo eccentric contractions. *Journal of Applied Physiology* 85: 58-67, 1998.
34. **Inserte J, Garcia-Dorado D, Hernando V, and Soler-Soler J.** Calpain-mediated impairment of Na^+/K^+-ATPase activity during early reperfusion contributes to cell death after myocardial ischemia. *Circulation Research* 97: 465-473, 2005.

35. **Irintchev A and Wernig A.** Muscle damage and repair in voluntarily running mice: strain and muscle differences. *Cell Tissue Research* 249: 509-521, 1987.
36. **Kieran D and Greensmith L.** Inhibition of calpains, by treatment with leupeptin, improves motorneuron survival and muscle function in models of motorneuron degeneration. *Neuroscience* 125: 427-439, 2004.
37. **Koh TJ and Escobedo J.** Cytoskeletal disruption and small heat shock protein translocation immediately after lengthening contractions. *American Journal of Cell Physiology* 286: C713-C722, 2004.
38. **Komatsu K, Inazuki K, Hosoya J, and Satoh S.** Beneficial effect of new thiol protease inhibitors, epoxide derivatives, on dystrophic mice. *Experimental Neurology* 91: 23-29, 1986.
39. **Lieber RL, Thornell L-e, and Fridén J.** Muscle cytoskeletal disruption occurs within the first 15 min of cyclic eccentric contraction. *Journal of Applied Physiology* 80: 278-284, 1996.
40. **Lovering RM and Deyne PGD.** Contractile function, sarcolemma integrity, and the loss of dystrophin after skeletal muscle eccentric contraction-induced injury. *American Journal of Cell Physiology* 286: C230-C238, 2004.
41. **Lowe DA, Warren GL, Hayes DA, Farmer MA, and Armstrong RB.** Eccentric contraction-induced injury of mouse soleus muscle: effect of varying $[Ca^{2+}]_o$. *Journal of Applied Physiology* 76: 1445-1453, 1994.
42. **Luzio JP, Poupon V, Lindsay MR, Mullock BM, Piper RC, and Pryor PR.** Membrane dynamics and the biogenesis of lysosomes (review). *Molecular Membrane Biology* 20: 141-154, 2003.
43. **Lynch GS, Fary CJ, and Williams DA.** Quantitative measurement of resting skeletal muscle $[Ca^{2+}]_i$ following acute and long-term downhill running exercise in mice. *Cell Calcium* 22: 373-383, 1997.
44. **McCully KK and Faulkner JA.** Injury to skeletal muscle fibers of mice following lengthening contractions. *Journal of Applied Physiology* 59: 119-126, 1985.
45. **Morgan DL.** New insights into the behavior of muscle during active lengthening. *Biophysical Journal* 57: 209-221, 1990.
46. **Proske U and Allen TJ.** Damage to skeletal muscle from eccentric exercise. *Exercise and Sport Science Reviews* 33: 98-104, 2005.
47. **Proske U and Morgan DL.** Muscle damage from eccentric exercise: mechanism, mechanical signs, adaptation and clinical applications. *Journal of Physiology* 537: 333-345, 2001.
48. **Raman S, Kelley MA, and Janssen PM.** Effect of muscle dimensions on trabecular contractile performance under physiological conditions. *European Journal of Physiology* 451: 625-630, 2006.
49. **Ray SK, Matzelle DC, Wilford GG, Hogan EL, and Banik NL.** E-64-d prevents both calpain upregulation and apoptosis in the lesion and penumbra following spinal cord injury in rats. *Brain Research Reviews* 867: 80-89, 2000.
50. **Ray SK, Matzelle DD, Wilford GG, Hogan EL, and Banik NL.** Cell death in spinal cord injury (SCI) requires *de novo* protein synthesis: calpain inhibitor E-64-d

provides neuroprotection in SCI lesion and penumbra. *Annals New York Academy of Sciences*: 436-449.
51. **Raynaud F, Fernandez E, Coulis G, Aubry L, Vignon X, Bleimling N, Gautel M, Benyamin Y, and Ouali A.** Calpain 1-titin interactions concentrate calpain 1 in the Z-band edges and in the N2-line region within the skeletal myofibril. *Federation of European Biochemical Societies Journal* 272: 2578-2590, 2005.
52. **Saido TC, Sorimachi Y, and Suzuki K.** Calpain: new perspectives in molecular diversity and physiological-pathological involvement. *Federation of American Societies for Experimental Biology Journal* 8, 1994.
53. **Solomon V and Goldberg AL.** Importance of the ATP-ubiquitin-proteasome pathway in the degradation of soluble and myofibril proteins in rabbit muscle extracts. *Journal of Biological Chemistry* 271: 26690-26697, 1996.
54. **Sorimachi Y, Imajoh-Ohmi S, Emori Y, Kawasaki H, Ohno S, Minami Y, and Suzuki K.** Molecular cloning of a novel mammalian calcium-dependent protease distinct from both m- and μ- types. *Journal of Biological Chemistry* 264: 20106-20111, 1989.
55. **Sorimachi Y, Saido TC, and Suzuki K.** New era of calpain research discovery of tissue-specific calpains. *Federation of European Biochemical Societies Letters* 343: 1-5, 1994.
56. **Spencer MJ, Croall DE, and Tidball JG.** Calpains are activated in necrotic fibers from mdx dystrophic mice. *Journal of Biological Chemistry* 270: 10909-10914, 1995.
57. **Spencer MJ and Tidball JG.** Calpain translocation during muscle fiber necrosis and regeneration in dystrophin-deficient mice. *Experimental Cell Research* 226: 264-272, 1996.
58. **Stelzer JE and Widrick JJ.** Effect of hindlimb suspension on the functional properties of slow an fast soleus fibers from three strains of mice. *Journal of Applied Physiology* 95: 2425-2433, 2003.
59. **Stracher A.** Calpain inhibitors as therapeutic agents in nerve and muscle degeneration. *Annals New York Academy of Sciences* 884: 52-59, 1999.
60. **Taillandier D, Combaret L, Pouch M-N, Samuels SE, Béchet, and Attaix D.** The role of ubiquitin-proteasome-dependent proteolysis in the remodeling of skeletal muscle. *Proceedings of the Nutrition Society* 63: 357-361, 2004.
61. **Takamure M, Murata K-y, Tamada Y, Azuma M, and Ueno S.** Calpain-dependent α-fodrin cleavage at the sarcolemma in muscle diseases. *Muscle Nerve* 32: 303-309, 2005.
62. **Tsuji T, Ohga Y, Yoshikawa Y, Sakata S, Abe T, Tabayashi N, Kobayashi S, Kohzuki H, Yoshida K-i, Suga H, Kitamura S, Taniguchi S, and Takaki M.** Rat cardiac contractile dysfunction induced by Ca^{2+} overload: possible link to the proteolysis of α-fodrin. *American Journal of Physiology-Heart and Circulatory Physiology* 281: H1286-H1294, 2001.
63. **Turk B, Turk D, and Turk V.** Lysosomal cysteine proteases: more than scavengers. *Biochimica et Biophysica Acta* 1477: 98-111, 2000.

64. **Verburg E, Murphy RM, Stephenson DG, and Lamb GD.** Disruption of excitation-contraction coupling and titin by endogenous Ca^{2+}-activated proteases in toad muscle fibers. *Journal of Physiology* 564: 775-789, 2005.
65. **Wang K, K. W.** Developing selective inhibitors of calpain. *Trends in Pharmacological Sciences* 11: 139-142, 1990.
66. **Wang K, McCarter R, Wright J, Beverly J, and Ramirez-Mitchell R.** Viscoelasticity of the sarcomere matrix of skeletal muscles: the titin-myosin composite filament is a dual-stage molecular spring. *Biophysical Journal* 64: 1161-1177, 1993.
67. **Warren GL, Hayes DA, Lowe DA, and Armstrong RB.** Mechanical factors in the initiation of eccentric contraction-induced injury in rat soleus muscle. *Journal of Physiology* 464: 457-475, 1993.
68. **Warren GL, Hayes DA, Lowe DA, Prior BM, and Armstrong RB.** Materials fatigue initiates eccentric contraction-induced injury in rat soleus muscle. *Journal of Physiology* 464: 477-489, 1993.
69. **Warren GL, Hayes DA, Lowe DA, Williams JH, and Armstrong RB.** Eccentric contraction-induced injury in normal and hindlimb-suspended mouse soleus and EDL muscles. *Journal of Applied Physiology* 77: 1421-1430, 1994.
70. **Warren GL, Ingalls CP, and Armstrong RB.** Temperature dependency of force loss in Ca^{2+} homeostasis in mouse EDL muscle after eccentric contractions. *American Journal of Physiology-Regulatory, Integrative, and Comparative Physiology* 282: R1122-R1132, 2002.
71. **Warren GL, Ingalls CP, Lowe DA, and Armstrong RB.** Excitation-contraction uncoupling: major role in contraction-induced muscle injury. *Exercise and Sport Science Reviews* 29: 82-87, 2001.
72. **Warren GL, Lowe DA, Hayes DA, Karwoski CJ, Prior BM, and Armstrong RB.** Excitation failure in eccentric contraction-induced injury of mouse soleus muscle. *Journal of Physiology* 468: 487-499, 1993.
73. **Widrick JJ, Romatowski JG, Norenberg KM, Knuth ST, Bain JLW, Riley DA, Trappe SW, Trappe TA, Costill DL, and Fitts RH.** Functional properties of slow and fast gastrocnemius muscle fibers after 17-day spaceflight. *Journal of Applied Physiology* 90: 2203-2211, 2001.
74. **Wood SA, Morgan DL, and Proske U.** Effects of repeated eccentric contractions on structure and mechanical properties of toad sartorius muscle. *American Journal of Cell Physiology* 265: C792-C800, 1993.
75. **Yoshida K-i, Inui M, Harada K, Saido TC, Sorimachi Y, Ishihara T, Kawashima S-i, and Sobue K.** Reperfusion of rat heart after brief ischemia induces proteolysis of calspectin (nonerythroid spectrin or fodrin) by calpain. *Circulation Research* 77: 603-610, 1995.